

Magnetic Resonance Dynamics via Fractional Bloch Equation: a Hybrid Computational Framework

Neetu Garg¹, Diptiranjana Biswal², Varsha R³

^{1,2,3}Department of Mathematics, National Institute of Technology Calicut, India

Email: neetu@nitc.ac.in

Abstract

Bloch equations are a powerful tool in describing the dynamics of nuclear magnetization in magnetic resonance phenomena. The fractional generalization of the Bloch equation effectively captures the anomalous relaxation and diffusion in porous, heterogeneous, and complex media. These equations describe how nuclear magnetization evolves under the influence of magnetic fields and relaxation processes. This work effectively employs a hybrid approach, the Laplace residual power series method, to investigate and analyze the fractional Bloch equation. A series solution is derived as the approximate solution for magnetization components. The influence of fractional order on each magnetization component in magnetization dynamics is analyzed and illustrated graphically. We conduct an error analysis to demonstrate the reliability and effectiveness of the proposed approach. The superiority of the suggested approach is shown using a comparative study with existing methods. The findings indicate the potential of the suggested approach as a reliable tool in understanding fractional magnetic resonance systems arising in applications such as NMR spectroscopy, MRI, MRF, and other complex heterogeneous materials.

1 Introduction

Fractional calculus has emerged as a powerful mathematical framework that extends the classical calculus and deals with integrals and derivatives of arbitrary order [1]. One of the key features of the fractional operators is their ability to incorporate the memory effect, in which the system's current state depends not only on current inputs but also on its entire past. This effect improves the modeling of real-life problems. This field is continuously evolving, and its relevance and applications in science and engineering are growing. Specifically, it has more significant applications in fields such as viscoelasticity, signal processing, biology, fluid dynamics, and control theory [2–5].

In 1946, Felix Bloch introduced the Bloch equations, which are macroscopic equations that help us to understand the magnetic resonance as a set of first-order differential equations [6]. Later, in 1956, Torrey added diffusion terms to these equations to study magnetization under the influence of shifting and relaxing magnetic fields [7]. The Bloch equations describe how nuclear magnetization evolves over time. They describe the spin system's relaxation dynamics by characterizing the time rate of change of magnetization. This system of equations has significant relevance in numerous scientific and engineering domains, particularly in applications such as nuclear magnetic resonance (NMR) [8], magnetic resonance imaging (MRI) [9], electron spin resonance (ESR) [10], and magnetic resonance fingerprinting (MRF) [11]. NMR imaging and spectroscopy technique is used to determine the structure of molecules. Scientists use it extensively in chemistry and biochemistry to understand how molecules are built and how they interact with each other. MRI is used to capture clear images of the interior of the human body. MRI is especially useful for examining the brain and detecting diseases such as cancer. ESR is used to study tiny particles called electrons in various materials. It also plays a role in developing quantum computers by enabling control over these electrons. Extremely accurate atomic clocks also use this technology to maintain precise timekeeping. This is crucial for applications like GPS, which rely on exact timing to provide accurate location information. MRF is a new and faster way to do MRI scans to get more detailed information about the tissues inside our body. The system of classical Bloch equations is given by [12]

$$\begin{cases} \frac{dM_x(t)}{dt} = \omega_0 M_y(t) - \frac{M_x(t)}{T_2}, \\ \frac{dM_y(t)}{dt} = -\omega_0 M_x(t) - \frac{M_y(t)}{T_2}, \\ \frac{dM_z(t)}{dt} = \frac{M_0 - M_z(t)}{T_1}, \end{cases} \quad (1)$$

with the initial state

$$M_x(0) = 0, \quad M_y(0) = 100, \quad M_z(0) = 0.$$

Here, $M_x, M_y,$ and M_z are the components of the magnetization vector M along the $x, y,$ and z directions, respectively. M_0 represent the equilibrium magnetization along the z -axis. The angular frequency ω_0 , measured in radians, $\omega_0 = \gamma B_0$ and $\omega_0 = 2\pi f_0$, where B_0 is the static magnetic field (z -component), f_0 is linear frequency measured in hertz, and γ is the gyromagnetic ratio. Then $\frac{\gamma}{2\pi} = \frac{f_0}{B_0} = 42.57$ MHz/Tesla for water protons. Here, T_1 and T_2 represent the spin lattice and spin-spin relaxation times, respectively. The longitudinal relaxation time T_1 characterizes the process by which the nuclear spins regain the thermal equilibrium with the surrounding lattice through energy transfer. In contrast, T_2 describes the time over which the spins lose coherence in the transverse plane due to spin-spin interaction. The values of T_1 and T_2 vary across different body tissues.

The system of equations (1) admits the following analytical solution

$$M_x(t) = e^{-t/T_2} [M_x(0) \cos(\omega_0 t) + M_y(0) \sin(\omega_0 t)],$$

$$M_y(t) = e^{-t/T_2} [M_y(0) \cos(\omega_0 t) - M_x(0) \sin(\omega_0 t)],$$

$$M_z(t) = M_z(0)e^{-t/T_1} + M_0 \left(1 - e^{-t/T_1}\right).$$

Taking the asymptotic limit $t \rightarrow \infty$, the steady state solution associated with (1) can be derived. Fractional Bloch equations are generalizations of the classical Bloch equations that capture memory effects, heterogeneity in the relaxation process, and complex magnetization dynamics. In this study, we investigate fractional Bloch equations described by [12]

$$D_t^\alpha M_x(t) = \omega_0 M_y(t) - \frac{M_x(t)}{T_2}, \quad (2)$$

$$D_t^\alpha M_y(t) = -\omega_0 M_x(t) - \frac{M_y(t)}{T_2}, \quad (3)$$

$$D_t^\alpha M_z(t) = \frac{M_0 - M_z(t)}{T_1}, \quad (4)$$

with initial state

$$M_x(0) = 0, \quad M_y(0) = 100, \quad \text{and} \quad M_z(0) = 0. \quad (5)$$

Here D_t^α denotes the Caputo fractional derivative operator of order $\alpha \in (0, 1]$ [1].

In 2008, Magin et al. introduced this fractional Bloch equation to describe the magnetization dynamics in porous, complex, and heterogeneous media [13]. This model enables the characterization of the anomalous relaxation and diffusion in such materials. Later, I. Petráš studied the behavior and stability analysis of the fractional Bloch equation [14]. In 2011, Bhalekar introduced the time delay concept in the fractional Bloch equation with [15]. Lately, many researchers have implemented mathematical methods for solving fractional Bloch equations, which include the operational matrix method [10, 16], homotopy perturbation method [12], Lagrange's polynomial interpolation [17], Laplace transform method [18], Sumudu transform method [19], fractional variational iteration method [20], analytical iterative method [21], residual power series methods [22, 23], etc.

The topic of solving fractional differential equations has attracted significant attention, leading to the development of a variety of analytical and numerical methods. Recently, some authors have proposed hybrid methods that are developed by combining an integral transform with traditional analytical methods. One such combination is the Laplace transform and the residual power series method, known as the Laplace residual power series method (LRPSM) [24]. This method delivers an accurate approximate solution as a convergent series. This method does not require perturbation, linearization, or discretization, unlike other existing methods. Recently, many scholars have employed the proposed technique to obtain solutions to a wide range of fractional differential equations, as shown in Refs. [25–28].

This paper explains the implementation of LRPSM to find approximate series solutions of the fractional Bloch equations. We convert the system of fractional differential equations in to an equivalent system of algebraic equations and determine the unknown coefficients in the series solution in the Laplace domain. We demonstrate a rigorous analysis of the obtained approximate solution of magnetization components through graphical illustrations. We discuss the phase-plane trajectories describing the transverse components of magnetization and the influence of fractional orders on the Bloch equations. Furthermore, to highlight the superiority of the proposed method, we present a comparative study with other existing methods.

This remainder of this paper is organized in the following manner: Section 2 presents preliminary concepts related to Caputo fractional derivative and the suggested method. In Section 3, we rigorously outlines the methodology of the suggested approach for deriving the solution of a system of equations. The detailed solution process for the fractional Bloch equation using LRPSM is discussed in Section 4. We analyze the numerical findings and compare them with other existing methods in Section 5. Finally, we conclude in Section 6.

2 Mathematical Preliminaries

This section is devoted to the fundamental definitions and features of the Caputo fractional derivative and the Laplace transform. Additionally, we recall theorems related to fractional power series.

Definition 1 (Caputo derivative). *The Caputo fractional derivative with order $\alpha > 0$ of the given function $\varphi(t)$, $t \in (a, b)$ and $m - 1 < \alpha \leq m$ ($m \in \mathbb{Z}^+$), is defined as [1]*

$$D_t^\alpha \varphi(t) = \frac{1}{\Gamma(m - \alpha)} \int_a^t (t - s)^{m - \alpha - 1} \varphi^{(m)}(s) ds.$$

Definition 2 (Laplace transform). *The Laplace transform of a piecewise continuous function $\varphi(t)$ of exponential order δ is defined as follows:*

$$\Phi(s) = \mathcal{L}\{\varphi(t)\} = \int_0^\infty e^{-st} \varphi(t) dt, \quad s > \delta.$$

The inverse Laplace transform of the function $\Phi(s)$ is defined as,

$$\varphi(t) = \mathcal{L}^{-1}\{\Phi(s)\} = \int_{\eta - i\infty}^{\eta + i\infty} e^{st} \Phi(s) ds, \quad \eta = \text{Re}(s) > 0.$$

Some characteristic features of the Laplace transform are listed below: [24]

1. $\lim_{s \rightarrow \infty} s\Phi(s) = \lim_{t \rightarrow 0} \varphi(t) = \varphi(0)$.
2. $\mathcal{L}\{D_t^\alpha \varphi(t)\} = s^\alpha \Phi(s) - \sum_{k=0}^{m-1} s^{\alpha-k-1} \varphi^{(k)}(0)$, $m - 1 < \alpha \leq m$.

Theorem 1. [24] *Let $\varphi(t)$ admits a fractional power series (FPS) representation about $t = 0$ given by*

$$\varphi(t) = \sum_{n=0}^{\infty} c_n t^{n\alpha}, \quad 0 < m - 1 < \alpha \leq m, \quad 0 \leq t < b. \quad (6)$$

Suppose $\varphi(t)$ is continuous and $D_t^{n\alpha} \varphi(t)$ exists and continuous on $t \in (0, b)$ for $n \geq 0$. Then the coefficients c_n in Eq. (6) take the form

$$c_n = \frac{D_t^{n\alpha} \varphi(0)}{\Gamma(n\alpha + 1)}, \quad n = 0, 1, 2, \dots$$

Theorem 2. [24] *Assume that the Laplace transform $\Phi(s) = \mathcal{L}\{\varphi(t)\}$ admits a FPS representation of the form*

$$\Phi(s) = \sum_{n=0}^{\infty} \frac{c_n}{s^{n\alpha+1}}, \quad 0 < \alpha \leq 1, \quad s > 0,$$

where $c_n = D_t^{n\alpha} \varphi(0)$. The inverse Laplace transform of the FPS of $\Phi(s)$ has the following form

$$\varphi(t) = \sum_{n=0}^{\infty} \frac{D_t^{n\alpha} \varphi(0)}{\Gamma(n\alpha + 1)} t^{n\alpha}, \quad 0 < \alpha \leq 1, \quad t \geq 0.$$

Theorem 3. [24] *Suppose $\Phi(s) = \mathcal{L}\{\varphi(t)\}$ have the FPS representation in the form $\Phi(s) = \sum_{n=0}^{\infty} \frac{c_n}{s^{n\alpha+1}}$, $0 < \alpha \leq 1$, and $\left| s \mathcal{L}\{D_t^{(n+1)\alpha} \varphi(t)\} \right| \leq M$ ($M \in \mathbb{R}^+$) on $0 \leq s \leq d$. Then, the remainder $\mathcal{R}_n(s)$ holds the following bound*

$$|\mathcal{R}_n(s)| \leq \frac{M}{s^{(n+1)\alpha+1}}, \quad 0 \leq s \leq d, \quad (d \in \mathbb{R}^+).$$

3 Methodology

This section briefly presents a concise overview of the LRPSM approach for a system of equations, which will be employed to derive an approximate solution to the fractional Bloch equation. For a detailed methodology, we consider a general system of ℓ fractional differential equations involving the Caputo derivatives of order $\alpha \in (0, 1]$

$$D_t^\alpha \varphi_i(t) = f_i(t, \varphi_1(t), \varphi_2(t), \dots, \varphi_\ell(t)), \quad t \geq 0, \quad i = 1, 2, \dots, \ell, \quad (7)$$

subject to the initial condition $\varphi_i(0) = \varphi_{i,0}$. Here, f_i 's are known continuous real-valued functions and φ_i denotes the unknown smooth functions to be determined. For each $i = 1, 2, \dots, \ell$, we follow the below stated steps.

Step 1: Perform the Laplace transform on Eqs. 7 and simplify using the initial condition. Then, we obtain

$$\Phi_i(s) = \frac{\varphi_{i,0}}{s} + \frac{1}{s^\alpha} \mathcal{L}\{f_i(t, \varphi_1(t), \varphi_2(t), \dots, \varphi_\ell(t))\}, \quad (8)$$

where $\Phi_i(s) = \mathcal{L}\{\varphi_i(t)\}$.

Step 2: Suppose that the solutions $\Phi_i(s)$ of the Eq. (8) admit the following series expansion

$$\Phi_i(s) = \sum_{n=0}^{\infty} \frac{c_{i,n}}{s^{n\alpha+1}}, \quad s > 0, \quad i = 1, 2, \dots, \ell. \quad (9)$$

The corresponding k -th truncated series, denoted by Φ_i^k , is given by,

$$\Phi_i^k(s) = \sum_{n=0}^k \frac{c_{i,n}}{s^{n\alpha+1}} = \frac{\varphi_{i,0}}{s} + \sum_{n=1}^k \frac{c_{i,n}}{s^{n\alpha+1}}, \quad s > 0, \quad i = 1, 2, \dots, \ell. \quad (10)$$

Step 3: Define the Laplace residual function $\mathcal{LRes}_{\Phi_i}(s)$ associated with $\Phi_i(s)$ and consider its k -th Laplace residual function $\mathcal{LRes}_{\Phi_i^k}(s)$ as follows

$$\begin{aligned} \mathcal{LRes}_{\Phi_i}(s) &= \Phi_i(s) - \frac{\varphi_{i,0}}{s} - \frac{1}{s^\alpha} \mathcal{L}\{f_i(t, \mathcal{L}^{-1}\{\Phi_1(s)\}, \mathcal{L}^{-1}\{\Phi_2(s)\}, \dots, \mathcal{L}^{-1}\{\Phi_\ell(s)\})\}, \\ \mathcal{LRes}_{\Phi_i^k}(s) &= \Phi_i^k(s) - \frac{\varphi_{i,0}}{s} - \frac{1}{s^\alpha} \mathcal{L}\{f_i(t, \mathcal{L}^{-1}\{\Phi_1^k(s)\}, \mathcal{L}^{-1}\{\Phi_2^k(s)\}, \dots, \mathcal{L}^{-1}\{\Phi_\ell^k(s)\})\}. \end{aligned} \quad (11)$$

Step 4: Multiply each side of Eq. (11) by $s^{k\alpha+1}$.

Step 5: Find all $c_{i,n}$ (for $n = 1, 2, 3, \dots$) by using

$$\lim_{s \rightarrow \infty} s^{k\alpha+1} \mathcal{LRes}_{\Phi_i^k}(s) = 0, \quad k = 1, 2, 3, \dots$$

Step 6: Determine $\Phi_i^k(s)$ by substituting the values of $c_{i,n}$ into the k -th approximate solution.

Step 7: Find the k -th approximate solution $\varphi_i^k(t)$ by taking the inverse Laplace transform of $\Phi_i^k(s)$.

4 LRPSM Implementation on the Fractional Bloch Equations

This section describes the implementation of the LRPSM on the fractional Bloch equations. Consider the system of equations (2)- (5). Suppose

$$\mathcal{L}\{M_x(t)\} = \mathcal{M}_x(s), \quad \mathcal{L}\{M_y(t)\} = \mathcal{M}_y(s), \quad \mathcal{L}\{M_z(t)\} = \mathcal{M}_z(s).$$

Apply Laplace transform to the system (2)-(4) and employing the initial condition, we obtain

$$\begin{aligned} \mathcal{M}_x(s) &= \frac{\omega_0}{s^\alpha} \mathcal{M}_y(s) - \frac{1}{T_2 s^\alpha} \mathcal{M}_x(s), \\ \mathcal{M}_y(s) &= \frac{100}{s} - \frac{\omega_0}{s^\alpha} \mathcal{M}_x(s) - \frac{1}{T_2 s^\alpha} \mathcal{M}_y(s), \\ \mathcal{M}_z(s) &= \frac{M_0}{T_1 s^{\alpha+1}} - \frac{\mathcal{M}_z(s)}{T_1 s^\alpha}. \end{aligned} \quad (12)$$

According to LRPSM, we assume that the functions $\mathcal{M}_x(s)$, $\mathcal{M}_y(s)$, and $\mathcal{M}_z(s)$ have the following FPS representations

$$\begin{aligned} \mathcal{M}_x(s) &= \sum_{n=0}^{\infty} \frac{\mathbf{a}_n}{s^{n\alpha+1}}, & \mathcal{M}_x^k(s) &= \sum_{n=0}^k \frac{\mathbf{a}_n}{s^{n\alpha+1}}, \\ \mathcal{M}_y(s) &= \sum_{n=0}^{\infty} \frac{\mathbf{b}_n}{s^{n\alpha+1}}, & \mathcal{M}_y^k(s) &= \sum_{n=0}^k \frac{\mathbf{b}_n}{s^{n\alpha+1}}, \\ \mathcal{M}_z(s) &= \sum_{n=0}^{\infty} \frac{\mathbf{c}_n}{s^{n\alpha+1}}, & \mathcal{M}_z^k(s) &= \sum_{n=0}^k \frac{\mathbf{c}_n}{s^{n\alpha+1}}, \end{aligned} \quad (13)$$

where \mathcal{M}_x^k , \mathcal{M}_y^k , and $\mathcal{M}_z^k(s)$ are the k -th truncated series of $\mathcal{M}_x(s)$, $\mathcal{M}_y(s)$, and $\mathcal{M}_z(s)$, respectively. Here,

$$\mathbf{a}_0 = \lim_{s \rightarrow \infty} s \mathcal{M}_x(s) = M_x(0) = 0, \quad \mathbf{b}_0 = \lim_{s \rightarrow \infty} s \mathcal{M}_y(s) = M_y(0) = 100, \quad \text{and} \quad \mathbf{c}_0 = \lim_{s \rightarrow \infty} s \mathcal{M}_z(s) = M_z(0) = 0, \quad (14)$$

Now, we define the Laplace residual functions of $\mathcal{M}_x(s)$, $\mathcal{M}_y(s)$, and $\mathcal{M}_z(s)$ as follows

$$\begin{aligned} \mathcal{LRes}_{\mathcal{M}_x}(s) &= \mathcal{M}_x(s) - \frac{\omega_0}{s^\alpha} \mathcal{M}_y(s) + \frac{1}{T_2 s^\alpha} \mathcal{M}_x(s), \\ \mathcal{LRes}_{\mathcal{M}_y}(s) &= \mathcal{M}_y(s) - \frac{\mathbf{b}_0}{s} + \frac{\omega_0}{s^\alpha} \mathcal{M}_x(s) + \frac{1}{T_2 s^\alpha} \mathcal{M}_y(s), \\ \mathcal{LRes}_{\mathcal{M}_z}(s) &= \mathcal{M}_z(s) - \frac{M_0}{T_1 s^{\alpha+1}} + \frac{1}{T_1 s^\alpha} \mathcal{M}_z(s). \end{aligned} \quad (15)$$

Thus, the corresponding k -th residual functions are given as

$$\begin{aligned} \mathcal{LRes}_{\mathcal{M}_x}^k(s) &= \mathcal{M}_x^k(s) - \frac{\omega_0}{s^\alpha} \mathcal{M}_y^k(s) + \frac{1}{T_2 s^\alpha} \mathcal{M}_x^k(s), \\ \mathcal{LRes}_{\mathcal{M}_y}^k(s) &= \mathcal{M}_y^k(s) - \frac{\mathbf{b}_0}{s} + \frac{\omega_0}{s^\alpha} \mathcal{M}_x^k(s) + \frac{1}{T_2 s^\alpha} \mathcal{M}_y^k(s), \\ \mathcal{LRes}_{\mathcal{M}_z}^k(s) &= \mathcal{M}_z^k(s) - \frac{M_0}{T_1 s^{\alpha+1}} + \frac{1}{T_1 s^\alpha} \mathcal{M}_z^k(s). \end{aligned} \quad (16)$$

To compute the value of \mathbf{a}_1 , \mathbf{b}_1 , and \mathbf{c}_1 , we consider $k = 1$ in Eq. (16) and utilize (13) to obtain

$$\begin{aligned} \mathcal{LRes}_{\mathcal{M}_x}^1(s) &= \left(\frac{\mathbf{a}_0}{s} + \frac{\mathbf{a}_1}{s^{\alpha+1}} \right) - \frac{\omega_0}{s^\alpha} \left(\frac{\mathbf{b}_0}{s} + \frac{\mathbf{b}_1}{s^{\alpha+1}} \right) + \frac{1}{T_2 s^\alpha} \left(\frac{\mathbf{a}_0}{s} + \frac{\mathbf{a}_1}{s^{\alpha+1}} \right), \\ \mathcal{LRes}_{\mathcal{M}_y}^1(s) &= \left(\frac{\mathbf{b}_0}{s} + \frac{\mathbf{b}_1}{s^{\alpha+1}} \right) - \frac{\mathbf{b}_0}{s} + \frac{\omega_0}{s^\alpha} \left(\frac{\mathbf{a}_0}{s} + \frac{\mathbf{a}_1}{s^{\alpha+1}} \right) + \frac{1}{T_2 s^\alpha} \left(\frac{\mathbf{b}_0}{s} + \frac{\mathbf{b}_1}{s^{\alpha+1}} \right), \\ \mathcal{LRes}_{\mathcal{M}_z}^1(s) &= \left(\frac{\mathbf{c}_0}{s} + \frac{\mathbf{c}_1}{s^{\alpha+1}} \right) - \frac{M_0}{T_1 s^{\alpha+1}} + \frac{1}{T_1 s^\alpha} \left(\frac{\mathbf{c}_0}{s} + \frac{\mathbf{c}_1}{s^{\alpha+1}} \right). \end{aligned} \quad (17)$$

Multiplying each equation of the system (17) with $s^{\alpha+1}$ and taking the limit $s \rightarrow \infty$, yields

$$\begin{aligned} \lim_{s \rightarrow \infty} s^{\alpha+1} \mathcal{LRes}_{\mathcal{M}_x}^1(s) &= \mathbf{a}_1 - \omega_0 \mathbf{b}_0 = 0, \\ \lim_{s \rightarrow \infty} s^{\alpha+1} \mathcal{LRes}_{\mathcal{M}_y}^1(s) &= \mathbf{b}_1 + \frac{\mathbf{b}_0}{T_2} = 0, \\ \lim_{s \rightarrow \infty} s^{\alpha+1} \mathcal{LRes}_{\mathcal{M}_z}^1(s) &= \mathbf{c}_1 - \frac{M_0}{T_1} = 0. \end{aligned} \quad (18)$$

Hence, we derive $\mathbf{a}_1 = \omega_0 \mathbf{b}_0$, $\mathbf{b}_1 = -\frac{\mathbf{b}_0}{T_2}$, and $\mathbf{c}_1 = \frac{M_0}{T_1}$. Thus, continuing in this manner for $k = 2, 3, 4, \dots$ we derive

$$\begin{aligned} \mathbf{a}_2 &= -\frac{2\omega_0 \mathbf{b}_0}{T_2}, \quad \mathbf{a}_3 = -\omega_0^3 \mathbf{b}_0 + \frac{3\omega_0 \mathbf{b}_0}{T_2^2}, \quad \mathbf{a}_4 = \frac{4\omega_0^3 \mathbf{b}_0}{T_2} - \frac{4\omega_0 \mathbf{b}_0}{T_2^3}, \quad \dots \\ \mathbf{b}_2 &= -\omega_0^2 \mathbf{b}_0 + \frac{\mathbf{b}_0}{T_2^2}, \quad \mathbf{b}_3 = \frac{3\omega_0^2 \mathbf{b}_0}{T_2} - \frac{\mathbf{b}_0}{T_2^3}, \quad \mathbf{b}_4 = \omega_0^4 \mathbf{b}_0 - \frac{6\omega_0^2 \mathbf{b}_0}{T_2^2} + \frac{\mathbf{b}_0}{T_2^4}, \quad \dots \end{aligned}$$

and

$$\mathbf{c}_2 = -\frac{M_0}{T_1^2}, \quad \mathbf{c}_3 = \frac{M_0}{T_1^3}, \quad \mathbf{c}_4 = -\frac{M_0}{T_1^4}, \quad \dots$$

By taking the inverse Laplace transform of \mathcal{M}_x , \mathcal{M}_y , and \mathcal{M}_z , we obtain approximate series solutions in the form

$$\begin{aligned} \mathring{M}_x(t) &= 100 \omega_0 \left(\frac{t^\alpha}{\Gamma(\alpha+1)} - \frac{2t^{2\alpha}}{T_2 \Gamma(2\alpha+1)} + \frac{3t^{3\alpha}}{T_2^2 \Gamma(3\alpha+1)} - \frac{\omega_0^2 t^{3\alpha}}{\Gamma(3\alpha+1)} + \dots \right), \\ \mathring{M}_y(t) &= 100 E_\alpha \left(-\frac{t^\alpha}{T_2} \right) - \frac{100 \omega_0^2 t^{2\alpha}}{\Gamma(2\alpha+1)} + \frac{100 \omega_0^2}{T_2} \left(\frac{2t^{2\alpha}}{\Gamma(3\alpha+1)} + \frac{t^{3\alpha}}{\Gamma(3\alpha+1)} \right) + \dots, \end{aligned}$$

and

$$\mathring{M}_z = M_0 \left(1 - E_\alpha \left(-\frac{t^\alpha}{T_1} \right) \right),$$

where $E_\alpha(t)$ denotes the Mittag-Leffler function of one parameter. Here, $\mathring{M}_x(t)$, $\mathring{M}_y(t)$, and $\mathring{M}_z(t)$ denote the approximate solutions of magnetization components $M_x(t)$, $M_y(t)$, and $M_z(t)$, respectively.

5 Results and Discussions

This section presents numerical results obtained using the proposed method and discusses the physical dynamics of the approximate solution. To assess the accuracy and reliability of the proposed method, two types of error measures are considered, as described below

$$\text{Absolute errors } \mathbf{e}_x(t) = \left| M_x(t) - \overset{\circ}{M}_x(t) \right|, \mathbf{e}_y(t) = \left| M_y(t) - \overset{\circ}{M}_y(t) \right|, \mathbf{e}_z(t) = \left| M_z(t) - \overset{\circ}{M}_z(t) \right|,$$

$$\text{Relative error} = \frac{\mathbf{e}_i(t)}{\overset{\circ}{M}_i(t)}, \text{ where } i \in \{x, y, z\}.$$

We assume $\omega_0 = 1$, $T_1 = 1$ (ms)^q, and $T_2 = 20$ (ms)^q. In Table 1, we consider the approximate solution by taking 10 terms for $\alpha = 1$. We observe that the approximate solution is consistent with the solution obtained by other methods. The exact and approximate values are closely same. We observe that this method is more efficient than other existing methods, which indicate the reliability of the suggested method.

Table 1: Comparison with existing methods.

	t	Exact solution	LRPSM	ARA-RPSM [22]	FVIM [20]	FHPTM [20]	Operational Matrix [10]	HPM [12]	ATIM [21]
$M_x(t)$	0.1	9.9335	9.9335	9.9335	9.9335	9.95256	9.9245	9.9335	9.9335
	0.3	29.1120	29.1120	29.1120	29.1120	29.6219	29.1080	29.1034	29.1034
	0.5	46.7589	46.7588	46.7588	46.7589	49.0948	46.7732	46.6823	46.6823
	0.7	62.2060	62.2060	62.2060	62.2074	68.5244	62.2180	61.8762	61.8762
	0.9	74.8859	74.8859	74.8859	74.8943	88.0717	74.8814	73.8911	73.8911
$M_y(t)$	0.1	99.0042	99.0042	99.0042	99.0042	99.0037	99.0213	99.0187	99.0030
	0.3	94.1113	94.1113	94.1113	94.1113	94.0731	94.1645	94.1837	94.0573
	0.5	85.5915	85.5915	85.5915	85.5914	85.2988	85.5689	85.5518	85.2445
	0.7	73.8536	73.8536	73.8536	73.8529	72.7400	73.7886	73.1630	72.6465
	0.9	59.4258	59.4258	59.4258	59.4215	56.4183	59.3742	57.0572	56.3451
$M_z(t)$	0.1	0.0952	0.0952	0.0952	0.0952	0.0952	0.0952	0.0952	0.0952
	0.3	0.2592	0.2592	0.2592	0.2592	0.2592	0.2592	0.2592	0.2592
	0.5	0.3935	0.3935	0.3935	0.3935	0.3935	0.3935	0.3935	0.3935
	0.7	0.5034	0.5034	0.5034	0.5034	0.5034	0.5034	0.5034	0.5034
	0.9	0.5934	0.5934	0.5934	0.5934	0.5934	0.5934	0.5934	0.5934

Table 2: Absolute and relative errors.

	t	Absolute Error	Relative Error
$M_x(t)$	0.1	0	0
	0.2	5.32907051820075e-14	2.70934046325674e-15
	0.3	3.76942921320733e-12	1.29480040762691e-13
	0.4	8.87325768417213e-11	2.32462326405266e-12
	0.5	1.02684083458371e-09	2.19603535751521e-11
$M_y(t)$	0.1	1.42108547152020e-14	1.43537961139099e-16
	0.2	5.68434188608080e-14	5.85824534945981e-16
	0.3	2.41584530158434e-12	2.56700770424182e-14
	0.4	5.85345105719171e-11	6.48349962837456e-13
	0.5	6.89183821123152e-10	8.05201269150381e-12
$M_z(t)$	0.1	5.55111512312578e-17	5.83329603774665e-16
	0.2	5.55111512312578e-16	3.06235901422036e-15
	0.3	4.34097202628436e-14	1.67487546296745e-13
	0.4	1.01674224595172e-12	3.08402811188705e-12
	0.5	1.17418297307381e-11	2.98417907788256e-11

The absolute and relative errors by taking 10 terms of series solution for $\alpha = 1$ are summarized in Table 2. We observe that both errors remain negligibly small throughout the considered interval. The absolute errors increase over time. The consistently small relative errors indicate that the method provides stable, reliable approximations for the magnetization components.

The influence of fractional orders on transverse magnetization components $M_x(t)$ and $M_y(t)$ is depicted in Figure 1. We observe that both transverse components exhibit damped oscillatory behavior over time, which is

a characteristic feature of transverse relaxation in the classical Bloch system. Moreover, the degree of damping is strongly influenced by the fractional order. As α decreases from 1, the damping increases and leads to a faster attenuation, particularly as time increases. The variation in decay behavior according to the fractional order highlights that the fractional Bloch system effectively delivers the memory-dependent relaxation effects.

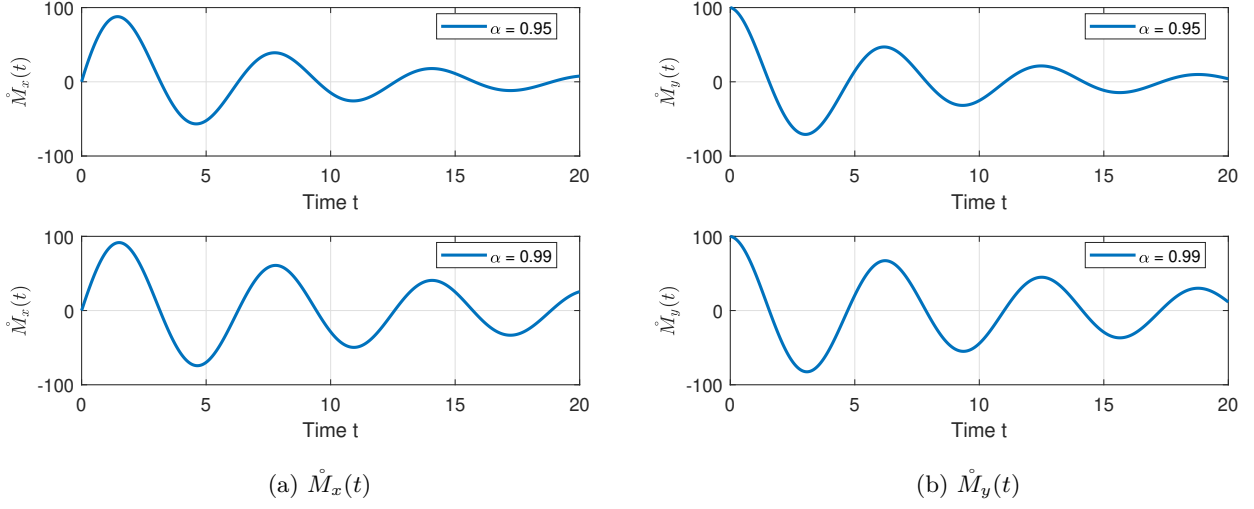


Figure 1: Time evolution of the transverse magnetization components $\dot{M}_x(t)$ and $\dot{M}_y(t)$ for different fractional orders (with 30 terms in series solution).

The variation of longitudinal magnetization component $M_z(t)$ with respect to time for various fractional orders in the relaxation dynamics is demonstrated in Figure 2. The magnetization increases monotonically and approaches to a steady state, indicating spin-lattice relaxation. A notable feature of the component $M_z(t)$ is observed near time $t \approx 1$, where all curves corresponding to different fractional orders intersect. Initially, we observe that $M_z(t)$ increases as α decreases. However, beyond this certain time, this trend reverse and $M_z(t)$ decreases with decrease in α .

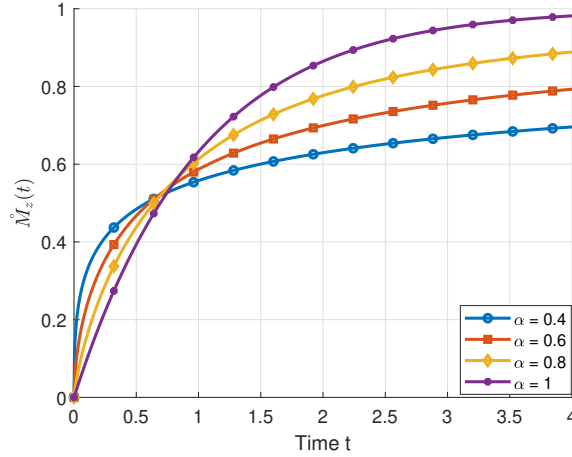


Figure 2: Time evolution of longitudinal magnetization component $\dot{M}_z(t)$ for different fractional orders (with 30 terms in the series solution).

Figure 3 demonstrate the comparison of our obtained solution of each magnetization components with the exact solution for the case $\alpha = 1$. The obtained solution coincides exactly with the approximate solution on the entire time domain. Moreover, it is notable that our obtained solution shows the oscillatory damping behavior in the same extent as of classical solution. This near-perfect overlap indicates that the proposed method accurately captures the transverse and longitudinal magnetic dynamics.

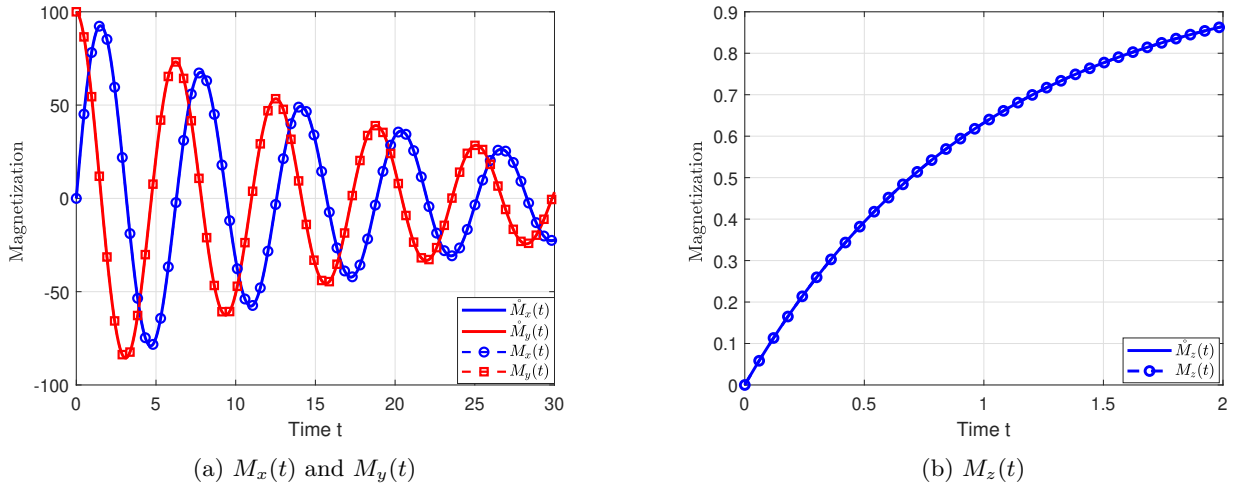
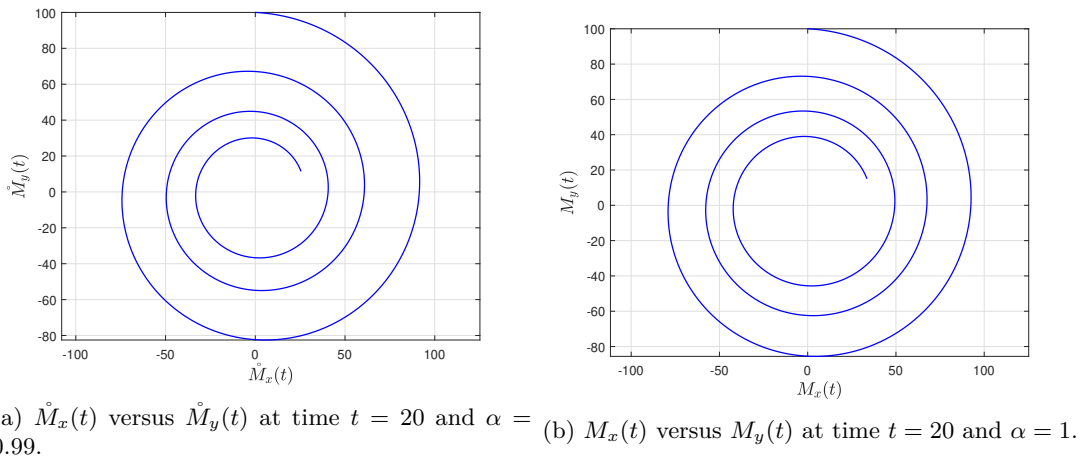
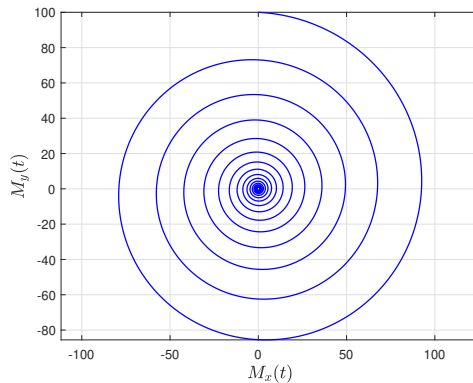


Figure 3: Comparison of exact and approximate solutions (with 50 terms in the series solution).

Figure 4 illustrates the phase plane representation of transverse components. The phase plane trajectories of transverse components exhibits a clear spiraling pattern towards the origin. This indicates the damped oscillatory behavior governed by relaxation effects. The trajectories of obtained approximate solution is illustrated in Figure 4a. The trajectories of analytical solution for $\alpha = 1$ at different times $t = 20$ and $t = 100$ are demonstrated in Figure 4b and 4c, respectively. It is visible that the solution undergoes complete damping as time progresses. Remarkably, we detect a slight deviation in the case of $\alpha = 0.99$, where the decay is comparatively slower, highlighting the presence of memory effect from fractional formulation. Moreover, the smoothness of obtained trajectories along with their close agreement with the expected physical behavior validate the effectiveness of proposed approach.



(a) $\dot{M}_x(t)$ versus $\dot{M}_y(t)$ at time $t = 20$ and $\alpha = 0.99$. (b) $M_x(t)$ versus $M_y(t)$ at time $t = 20$ and $\alpha = 1$.



(c) $M_x(t)$ versus $M_y(t)$ at time $t = 100$ and $\alpha = 1$.

Figure 4: Phase plane representation of transverse components (with 30 terms in the series solution).

We demonstrate the absolute error associated with each magnetization component in Figure 5. Here, we take approximate solutions up to the 4th, 7th, and 10th terms. The significant influence of the number of terms in the approximate solution on absolute errors is shown. We observe that the magnitude of error reduces remarkably as the number of terms increases, indicating convergence of the obtained solution. Moreover, the absolute error over the considered time interval is negligibly small, which highlighting the effectiveness and precision of the proposed method.

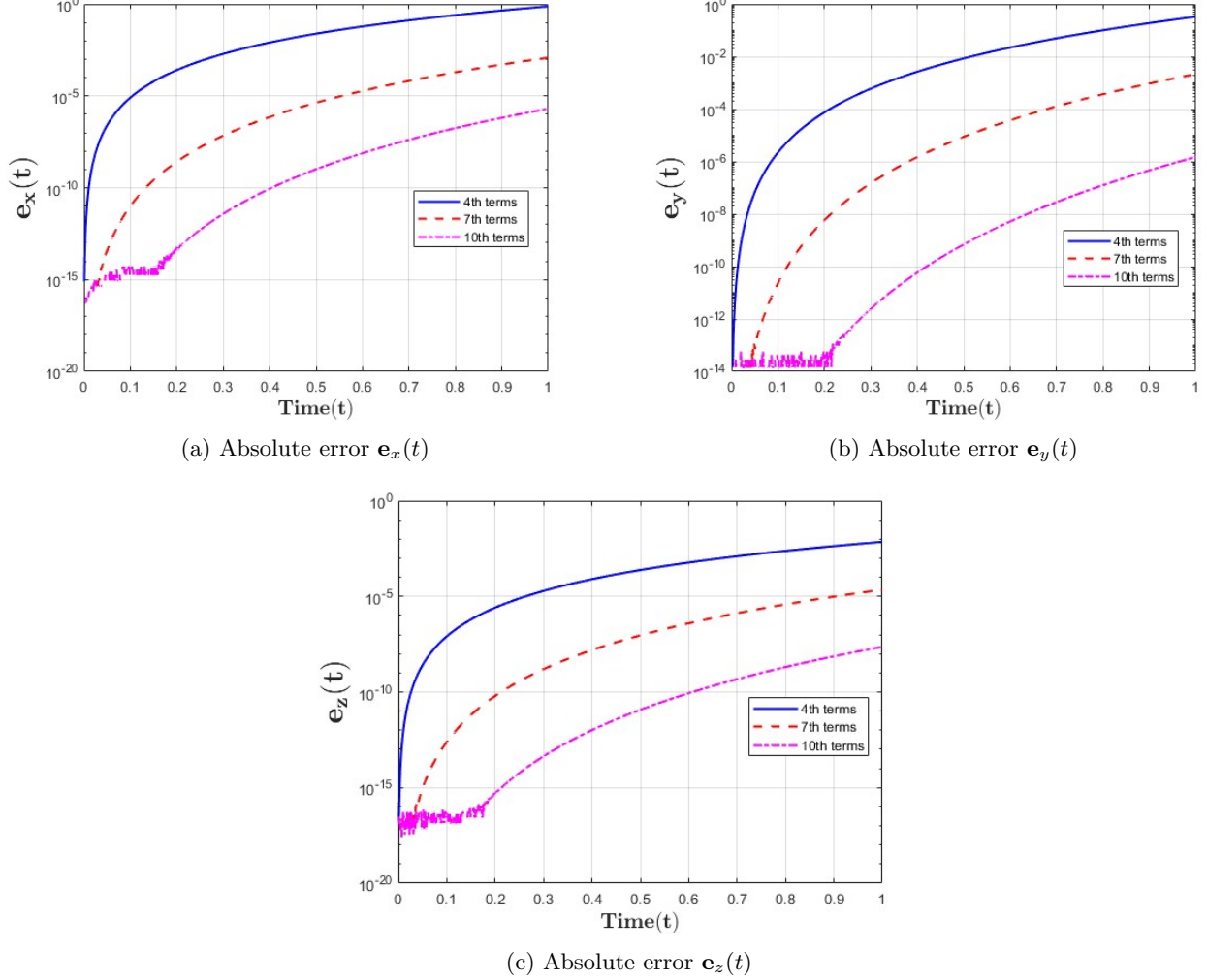


Figure 5: Comparison of absolute errors in $\dot{M}_x(t)$, $\dot{M}_y(t)$, and $\dot{M}_z(t)$ with different number of terms in approximate solution.

6 Conclusion

This work focuses on developing the approximate solution to the fractional Bloch equations using a hybrid approach, the Laplace-residual power series method. This method integrates the Laplace transform with the conventional residual power series approach. The conversion of the fractional Bloch equation into a system of algebraic equations is carried out by operating the Laplace transform. In contrast to the conventional residual power series method, this series solution approach does not need the computation of fractional derivatives. Instead, this method depends on the simple limiting process to extract the unknown coefficients. Also, unlike the other approaches for solving the fractional Bloch equation, this method does not require perturbation or discretizations. The obtained solution keeps a good agreement with the exact solution for all magnetization components. The absolute and relative error analyses demonstrate the high level of accuracy of the suggested method. Furthermore, the phase-plane trajectory illustrates the evolution of the magnetization vector and highlight the impact of fractional order parameter on the relaxation dynamics of the Bloch system. These results indicate that LRPSM is an efficient and reliable technique for studying fractional Bloch models encountered in magnetic resonance phenomena.

Acknowledgments

The authors would like to sincerely thank the anonymous editors and reviewers for their suggestions. Varsha R is supported by the University Grant Commission of India.

References

- [1] Igor Podlubny. *Fractional differential equations: an introduction to fractional derivatives, fractional differential equations, to methods of their solution and some of their applications*, volume 198. Elsevier, 1998.
- [2] T. F. Nonnenmacher and R. Metzler. Applications of fractional calculus ideas to biology. In *Applications of Fractional Calculus in Physics*. World Scientific, 1998.
- [3] J Tenreiro Machado, Virginia Kiryakova, and Francesco Mainardi. Recent history of fractional calculus. *Communications in nonlinear science and numerical simulation*, 16(3):1140–1153, 2011.
- [4] Kenneth S Miller and Bertram Ross. *An introduction to the fractional calculus and fractional differential equations*. Wiley, 1993.
- [5] Kai Diethelm and Neville J Ford. Analysis of fractional differential equations. *Journal of Mathematical Analysis and Applications*, 265(2):229–248, 2002.
- [6] Felix Bloch. Nuclear induction. *Physical Review*, 70:460–474, 1946.
- [7] Henry C Torrey. Bloch equations with diffusion terms. *Physical review*, 104(3):563, 1956.
- [8] Harendra Singh and Amit Kumar Singh. Numerical simulation for fractional Bloch equation arising in nuclear magnetic resonance. *Nonlinear Studies*, 28(2), 2021.
- [9] Arijit Hazra, Gert Lube, and Hans-Georg Raumer. Numerical simulation of Bloch equations for dynamic magnetic resonance imaging. *Applied Numerical Mathematics*, 123:241–255, 2018.
- [10] Harendra Singh. Operational matrix approach for approximate solution of fractional model of Bloch equation. *Journal of King Saud University - Science*, 29(2):235–240, 2017.
- [11] Haifeng Wang, Lixian Zou, Huihui Ye, Shi Su, Yuchou Chang, Xin Liu, and Dong Liang. Application of time-fractional order Bloch equation in magnetic resonance fingerprinting. In *2019 IEEE 16th International Symposium on Biomedical Imaging (ISBI 2019)*, pages 1704–1707. IEEE, 2019.
- [12] Sunil Kumar, Naeem Faraz, and Khosro Sayevand. A fractional model of Bloch equation in nuclear magnetic resonance and its analytic approximate solution. *Walailak Journal of Science and Technology*, 11(4):273–285, 2014.
- [13] Richard Magin, Xu Feng, and Dumitru Baleanu. Solving the fractional order bloch equation. *Concepts in Magnetic Resonance Part A*, 34A(1):16–23, 2009.
- [14] Ivo Petraš. Modeling and numerical analysis of fractional-order Bloch equations. *Computers & Mathematics with Applications*, 61(2):341–356, 2011.
- [15] Sachin Bhalekar, Varsha Daftardar-Gejji, Dumitru Baleanu, and Richard Magin. Fractional Bloch equation with delay. *Computers & Mathematics with Applications*, 61(5):1355–1365, 2011.
- [16] R.C. Mittal and Sapna Pandit. A numerical algorithm to capture spin patterns of fractional Bloch nuclear magnetic resonance flow models. *Journal of Computational and Nonlinear Dynamics*, 14(8):081001, 2019.
- [17] Ali Akgül, Ishfaq Ahmad Mallah, and Subhash Alha. New aspects of Bloch model associated with fractal fractional derivatives. *Nonlinear Engineering*, 10(1):323–342, 2021.
- [18] ASV Ravi Kanth and Neetu Garg. Analytical solutions of the bloch equation via fractional operators with non-singular kernels. In *Applied Mathematics and Scientific Computing: International Conference on Advances in Mathematical Sciences, Vellore, India, December 2017-Volume II*, pages 37–45. Springer, 2019.
- [19] Jagdev Singh, Devendra Kumar, and Dumitru Baleanu. New aspects of fractional Bloch model associated with composite fractional derivative. *Mathematical Modelling of Natural Phenomena*, 16:10, 2021.

- [20] Amit Prakash, Manish Goyal, and Shivangi Gupta. A reliable algorithm for fractional Bloch model arising in magnetic resonance imaging. *Pramana*, 92:1–10, 2019.
- [21] Akshey and Twinkle R Singh. Approximate-analytical iterative approach to time-fractional Bloch equation with Mittag–Leffler type kernel. *Mathematical Methods in the Applied Sciences*, 47(8):7028–7045, 2024.
- [22] B. Bala Sai Sankar and P. Karunakar. Computational technique for the solution of time-fractional Bloch equations with uncertain relaxation times. *Journal of Vibration Engineering & Technologies*, 13:545, 2025.
- [23] Ved Prakash Dubey, Jagdev Singh, Ahmed M. Alshehri, Sarvesh Dubey, and Devendra Kumar. Forecasting the behavior of fractional order Bloch equations appearing in NMR flow via a hybrid computational technique. *Chaos, Solitons & Fractals*, 164:112691, 2022.
- [24] Tareq Eriqat, Ahmad El-Ajou, Moa’ath N. Oqielat, Zeyad Al-Zhour, and Shaher Momani. A new attractive analytic approach for solutions of linear and nonlinear neutral fractional pantograph equations. *Chaos, Solitons & Fractals*, 138, 2020.
- [25] Sanjeev Yadav, Ramesh Kumar Vats, and Anjali Rao. Constructing the fractional series solutions for time-fractional K-dV equation using Laplace residual power series technique. *Optical and Quantum Electronics*, 56(5):721, 2024.
- [26] Fares Bekhouche, Iqbal M Batiha, Ouidad Boulakour, Radwan M Batyha, Ahmed Bouchenak, and Shaher Momani. Coupling Laplace transform with residual power series: A novel route to enhance nonlinear time-fractional Whitham–Broer–Kaup models. *WSEAS Transactions on Mathematics*, 24:694–706, 2025.
- [27] Sanjeev Yadav, Ramesh Kumar Vats, and Anjali Rao. Application of extended residual power series method for time-fractional Zakharov–Kuznetsov equations in ocean-based coastal wave. *Pramana*, 99(3):97, 2025.
- [28] Neetu Garg and Varsha R. On a class of multi-dimensional non-linear time-fractional fokker-planck equations capturing brownian motion. *ArXiv*, 2026.